Palaeogeography, Palaeoclimatology, Palaeoecology 414 (2014) 493–499

Contents lists available at ScienceDirect

Palaeogeography, Palaeoclimatology, Palaeoecology

journal homepage: www.elsevier.com/locate/palaeo

On porosity of archeological bones II. Textural characterization of Mesoamerican human bones

Josefina Mansilla [a], Carlos Moreno-Castilla [b], Pedro Bosch [c,*], Inmaculada Alemán [d], Carmen Pijoan [a], Miguel Botella [d]

[a] Dirección de Antropología Física, Instituto Nacional de Antropología e Historia, Gandhi s/n, Polanco, 11560 México D.F., Mexico
[b] Departamento de Química Inorgánica, Facultad de Ciencias, Universidad de Granada, 18002 Granada, Spain
[c] Instituto de Investigaciones en Materiales, Universidad Nacional Autónoma de México, 04510 México D.F., Mexico
[d] Laboratorio de Antropología, Facultad de Medicina, Universidad de Granada, 18012 Granada, Spain

ARTICLE INFO

Article history:
Received 31 March 2014
Received in revised form 11 August 2014
Accepted 26 August 2014
Available online 6 September 2014

Keywords:
Syphilis
Treponematosis
BET
SAXS
SEM
Taphonomy

ABSTRACT

Human bone porosity may be an indicator of many bone diseases but it can also reflect the influence of *postmortem* alterations. The usually reported values for textural parameters, such as specific surface area or porosity of archeological bones, are not consistent as pathology and taphonomy may alter bone morphology at nano and/or micrometrical levels. To illustrate those points, four archeological human bones were chosen; they differ in the environment where they were found and on their attributed diseases.
Complementary analysis techniques commonly mentioned in material science were used to characterize the chosen samples: gas adsorption, small angle X-ray scattering and scanning electron microscopy. It is shown that, even if the differences between human pathological and healthy bones can be clear in fresh materials, such alterations may be masked by taphonomy in archeological bones.

1. Introduction

Bone is a composite material constituted by an organic non crystalline protein, collagen, and a crystalline inorganic component, mineral hydroxyapatite (Weiner and Traub, 1992; Labastida Pólito et al., 2006), arranged in a complex internal and external structure which generates some porosity. Porosity as part of healthy human bone microarchitecture is due to numerous channels such as Harvesian and Volkmann canals averaging about 50 μm in diameter, osteocytic voids (*quasi* ellipsoidal and a few μm size) and canaliculi (diameter of approximately 200 μm). However, porosity varies depending on type or abnormal bone tissue; for instance, beneath the periosteum as a response to infection and age. The cortical porosity increases from *ca.* 8% for young individuals up to 24–28% for elder individuals. Harvesian canals increase significantly with age whereas lacuna porosity decreases slightly. The microstructure of bone tissues clearly influences its mechanical properties, porosity and, ultimately, its resistance to postmortem degradation (Wang and Ni, 2003; Turner-Walker, 2008).

Furthermore, many skeletal diseases, according to their acute or chronic process, can rapidly form woven bone that is poorly organized and always has a porous appearance due to the loose organization of the mineralized osteoid fibers, and tends to contain more vascular spaces than compact bone (Ortner, 2008). Pathological conditions as periostosis, osteoporosis or treponematosis, among others, are well known for their impact on bone pores (Waldron, 2009). Then, bone porosity can be also due to the individual response (according to sex, age and immune reaction), to taphonomy (interaction of bone with soil, degradation) and to different diseases such as treponematosis, anemia, or osteoporosis (Walker et al., 2009). It is thus tempting to use porosity as an indicator of age or as a possible indicator of pathology.

However, after burial, external processes may alter the texture and the morphology of the skeleton. In previous works, it has been shown how the role of climate and chronology may define diagenetic pathways (Gutierrez, 2001). For instance, habits, such as covering human remains with pigment can alter the preservation and the microscopical morphology of skeletons buried in the Maya zone (Cervini-Silva et al., 2013). Among those modifications, texture is one of the most altered features. Taphonomy, either through natural or human processes, modifies specific surface area and pore size distribution. Taphonomic alteration acts at different levels. Porosity is linked to the rearrangement of the crystal structure (Roberts et al., 2002; Bosch et al., 2011). It, then, varies depending on the degree of bone degradation.

* Corresponding author at: Instituto de Investigaciones en Materiales, Universidad Nacional Autónoma de México, Circuito Exterior, 04510 México D.F., Mexico. Tel.: +56 22 46 56.
E-mail address: croqcroq@hotmail.com (P. Bosch).

http://dx.doi.org/10.1016/j.palaeo.2014.08.029
0031-0182/

The problem is then difficult, as it depends also on the measurement technique. A review of the anthropological and archeological references reveals that results obtained with the current methodologies to measure specific surface area and pore size distributions are contradictory as they may depend on the used technique. Experiments with small angle X-ray scattering (SAXS) (Hiller and Wess, 2006; Pijoan et al., 2007) or nuclear magnetic resonance (NMR) (Wang and Ni, 2003) determine the external and internal porosity; they can differ from gas adsorption method, which, definitely, is the most direct technique to evaluate texture (Sing, 2001; Smith et al., 2008). Indeed, when a gas or vapor phase is brought into contact with a solid, part of it is taken up and remains on the outside attached to the surface. In physisorption (physical adsorption), there is a weak Van der Waals attraction between the adsorbate and the solid surface. The technique based on those principles is a useful tool to determine specific surface area, pore size distribution and porosity (Rouquerol et al., 1999), but it is related only to pores accessible to gases, i.e. open porosity.

In this work, we chose to study and compare bones, which at first glance, i.e. by macroscopic criteria, are modified in different degrees by taphonomy or treponematosis. The results obtained with gas adsorption are compared with those provided by scanning electron microscopy and small angle X-ray scattering. The final purpose is to compare textural evaluations at nano-metric and macro-metric levels and to show how difficult it is to establish, in archeological bones modified by taphonomy, a clear correlation between porosity and osteopathology. Only four extreme samples were chosen. Indeed, the taphonomy in a site as Tlatelolco (Mansilla et al., 2003), which was an island in the salted lake of Texcoco must be different than the expected one in a cave as Cueva de la Candelaria, located in a semi desert zone of North Mexico. The remains found in Cueva de la Candelaria are known as one of the best-preserved skeletal collections, with organic material present (soft tissue), showing evidence of severe lesions of treponematosis (Mansilla and Pijoan, 2005).

2. Experimental

2.1. Archeological context

The island of Tlatelolco in the Northern part of the Lake of Texcoco (Fig. 1) was occupied by a Náhuatl speaking group who settled there in the 13th century. The city of Tenochtitlán (actual Mexico City) was largely dependent on the market of Tlatelolco, the most important site of commerce in the area. The place was very humid and temperatures could vary from 0 to 35 °C although most of the time it was ca. 25 °C.

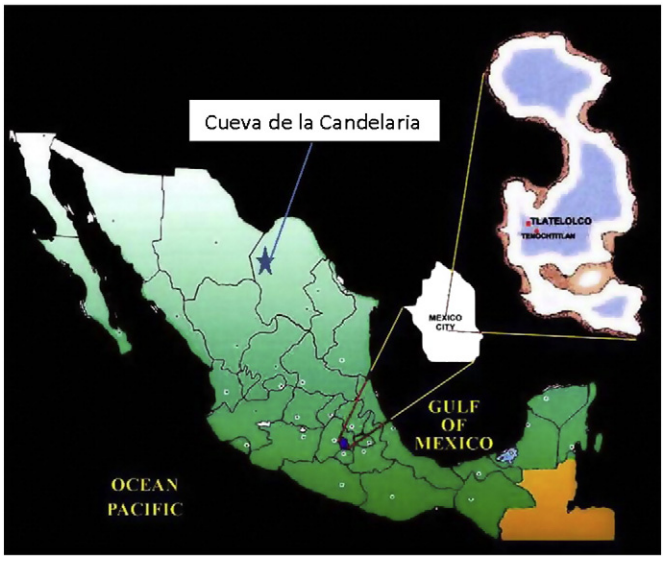

Fig. 1. Location of Tlatelolco and Cueva de la Candelaria. Tlatelolco, the twin city of Tenochtitlan, was settled at the Precolumbian Texcoco Lake, now Mexico City and the Cueva de la Candelaria is situated in North Mexico.

Instead, the Cueva de la Candelaria was chosen by a semi-nomadic group of mainly hunter–gatherers to deposit their dead from 800 to 1200 A.D. More than 4000 objects, 200 human remains, and many organic materials have been collected, as the microclimate in the cave propitiates at least partial mummification. The Cueva de la Candelaria is in the Sierra de la Candelaria (Coahuila) where the weather is very dry; it is, indeed, one of the driest and hottest of Mexico (Fig. 1).

The osteological sample was chosen to compare normal with morphologically altered bones by treponematosis. The term treponematosis is described by Powell and Cook (2005) as a set of four similar diseases known as venereal syphilis, endemic syphilis (bejel), yaws, and pinta. This family of diseases is caused by *Treponema* infection. One of the four diseases (pinta), is due to *Treponema carateum*, and produces lesions of the skin only. The other three syndromes can affect the skeletal system and other organs. They are associated with different subspecies of *Treponema pallidum*. The three syndromes of treponematosis that affect the skeleton (syphilis, bejel and yaws) produce specific lesions that could, in some cases, be considered to be pathognomonic of treponematosis (Powell and Cook, 2005). Ortner (2008) mentions that some efforts have been made to distinguish between the three skeletal manifestations of the three syndromes of treponematosis affecting the skeleton. Slight differences may be apparent in the adequate skeletal samples but he mentions that this research remains to be done. Hackett (1976) studied and described the cranial lesions and their developmental stages; the classic macroscopic appearance of skull vault lesions is *caries sicca*, a crater-like lesion with central destructive *focus* and reactive, compact bone formation on the margins of the lesion. The combination of a crater like lesion with the radiating lines of active lytic lesions, remodeling, and scarring is pathognomonic of treponemal infection (Ortner, 2008; Pinhasi and Mays, 2008; Waldron, 2009). Such features together with the prevalence of the total individuals affected may be used to infer if a bone is affected by treponematosis.

Still, Hackett (1976) cautions against attempts to differentiate syphilis, yaws, and treponarid (endemic syphilis) based upon isolated dry bones specimens, noting in his summary that the bone lesions of these closely related diseases cannot, at present, be separated. Still, they may be useful to make differential diagnosis between treponematosis and other diseases, such as tuberculosis, pyogenic osteomyelitis, chronic ulcers or Paget's disease. Periosteal reactive bone formation such as woven bone lesions remodeled into compact bone and, destructive lesions on the diaphyseal long bone surface characterizes the abnormalities apparent in the apendicular skeleton (Ortner, 2008). On bones near the surface such as the tibia, this alteration is characteristic of skeleton collections with a diagnosis of treponematosis (Waldron, 2009).

2.2. Samples

In Table 1, the labeling, the origin of the samples, the type of bone and the apparent disease following the macroscopic criteria previously exposed are presented. The samples were ground for Small Angle X-ray Scattering (SAXS) and Gas Adsorption measurements. In Scanning Electron Microscopy- Energy Dispersive X-ray Spectroscopy (SEM-EDS), a flake of the material was characterized to maintain the external surface structure.

2.3. Characterization methods

All bones were studied by nitrogen adsorption–desorption isotherms at −196 °C, scanning electron microscopy and small angle X-ray scattering. The adsorption desorption isotherms were obtained with a Quadrasorb automatical equipment provided by Quantachrome. Samples

Table 1
Mexican human bone samples; labeling and origin.

Type of bone	Origin classification	Labeling	Macroscopic condition[a]
Right tibia	Cueva de la Candelaria #19 CP expl. 1953–56	MC-tibia-s	Treponematosis
	Tlatelolco caja 353 TS	MT-tibia-h	Normal appearance
Metacarpal bone	Tlatelolco ent.C 1985	MT-metacarpal-s	Treponematosis
Left fibula	Cueva de la Candelaria #13 CS	MC-fibula-h	Normal appearance

[a] Following the criteria of Mays (2008) and Waldron (2009).

were previously outgassed overnight at 110 °C with a dynamical vacuum of *ca.* 10^{-6} mbar. Scanning electron microscopy studies were performed with a Leica Stereoscan 440 microscope. The samples were previously sputtered with gold to avoid charge problems. The EDS results correspond to an area of 80 × 70 μm. SAXS experiments were performed with a Kratky camera. The powdered sample was introduced into a capillary tube. Intensity I(h) was measured for 9 min in order to obtain good quality statistics. The SAXS data were processed with the ITP program (Glatter and Gruber, 1993).

3. Results

3.1. Gas adsorption

In gas adsorption, the dynamic phase equilibrium established is usually expressed in terms of partial pressure of the adsorbate per unit mass of the adsorbent. If the data are taken over a range of gas pressures at a constant temperature, a plot of gas loading on the adsorbent versus partial pressure of the gas can be made. Such a plot is called the adsorption isotherm. For pure gases, experimental physical adsorption isotherms have shapes that are classified into 5 types. By far the most common are types I, II and IV, each one corresponds to a particular interaction of the gas molecules and the solid adsorbate. For instance, an inherent property of type I isotherms is that adsorption is limited to the completion of a single monolayer of adsorbate at the adsorbent surface. Type I isotherms are observed for the adsorption of gases on microporous solids whose pore sizes are not much larger than the molecular diameter of the adsorbate. An example is the adsorption of oxygen on carbon black at −183 °C.

The samples from the Cueva de la Candelaria did not adsorb nitrogen at the used experimental conditions; therefore, they are not porous; i.e. pores are not accessible to gases, but this result has to be compared to SAXS measurements which include also closed porosity (porosity which is not accessible to gases). The shape of nitrogen adsorption isotherms for Tlatelolco samples corresponds to the well-known irreversible type II or IIb; a hysteresis loop type H3 as defined by IUPAC is present (Rouquerol et al., 1999) (Fig. 2). This type of hysteresis loop corresponds to adsorbents constituted by aggregates of platy particles or adsorbents with slit shaped mesopores. It is typical of clays and, natural or synthetic, hydroxyapatite (El Shafei et al., 2004).

The surface area was determined using the BET equation (Table 2). The Tlatelolco samples were not microporous (pores less than 2 nm) as far as gas adsorption is concerned. However, the total pore volume, Vp, could be obtained from the amount of (liquid) nitrogen adsorbed at a relative pressure $p/p_0 = 1$. If mesopores are slit-like, their mean width may be estimated using the equation $d = 2V_P/S_{BET}$. In sample MT-tibia-h, it turned out to be 7.42 nm and in MT-metacarpal-s it was 5.44 nm; these values are the same as the sizes expected for canaliculi.

3.2. Small angle X-ray diffraction

If the relevant structural features are at superatomic level, from a few tenths up to about 100 nm, small-angle X-ray scattering (SAXS) is the most widely used technique (Craievich, 2002). In this characterization technique, not often mentioned in archeological bone studies, the X-ray scattering intensity is experimentally determined as a function of the scattering vector q whose modulus is given by $q = (4\pi/\lambda).\sin\theta$, where λ is the X-ray wavelength and θ is half the scattering angle between the directions of the scattered and transmitted beams. The scattered intensity is due to differences in electron density, for instance pores in a continuous medium or dense particles or both. It is difficult to decide which one of those heterogeneities is responsible of the observed scattering due to Babinet's theorem which states that the X-ray scattering intensity, I(q), of a small particle with homogeneous electron density cannot be distinguished from the scattering of an infinite large sample with the same electron density but with a cut-out of the size of the small particle. The angular deviation of scattered rays has an inverse relationship with size. Then, the position and shape of an X-ray scattering curve can be used to determine the average shape and size of heterogeneities in a sample. The analysis of the SAXS curve provides the gyration radius, the size distribution, the shape and the fractal dimension of the scattering heterogeneities (Guinier and Fournet, 1955; Kataoka et al., 1993, 1994; Wess et al., 2001a,b; Vinogradova et al., 2003).

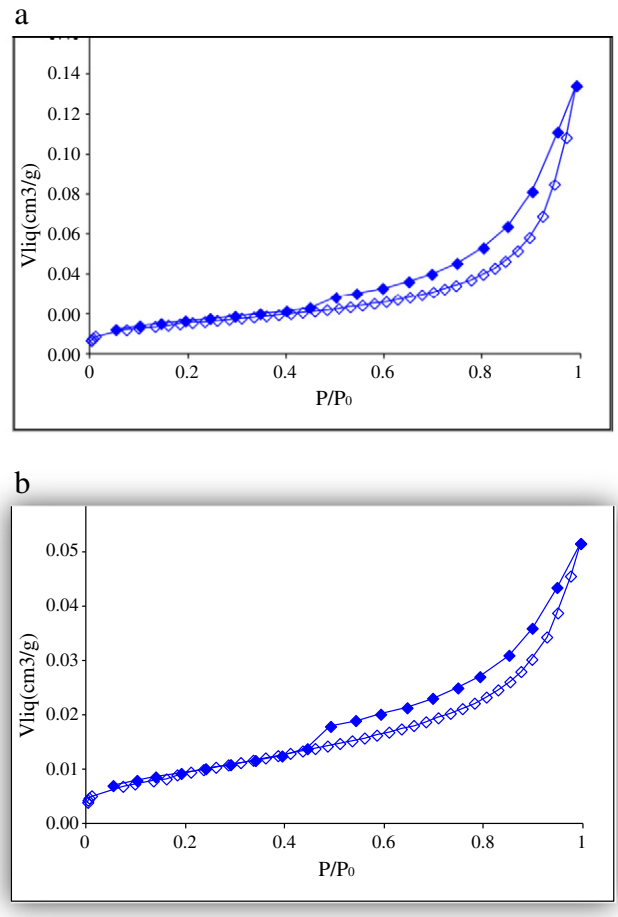

Fig. 2. Comparison of the N2 adsorption–desorption isotherms at −196 °C of the Tlatelolco samples a) MT-tibia-h and b) MT-metacarpal-s.

Table 2
Textural features of the Mesoamerican bones as determined by gas adsorption.

Bone type	Origin	Labeling	Bone condition	S_{BET} ($m^2/g \pm 0.7$)	V_p ($cm^3/g \pm 0.01$)
Right tibia	Cueva de la Candelaria #19 CP expl. 1953–56	MC-tibia-s	Treponematosis	<2[a]	–
	Tlatelolco Caja 353 TS	MT-tibia-h	Normal appearance	35	0.13
Metacarpal	Tlatelolco ent. C 1985	MT-metacarpal-s	Treponematosis	22	0.05
Left fibula	Cueva de la Candelaria #13 CS	MC-fibula-h	Normal appearance	<2[a]	–

[a] This is the lowest S_{BET} value that can be determined with the equipment and available amount of sample used.

The diameters corresponding to the peaks found in the heterogeneity size distributions, the shape of heterogeneities, and the gyration radii are compared in Table 3. Heterogeneity size distributions of the studied Mesoamerican bones are broad, from D = 0.5 to 5 nm (Fig. 3). The distributions of healthy archeological bones (MC-fibula-h and MT-tibia-h) are similar, with three peaks at 1.2, 2.7 and 4.4 nm. The peak at 4.4 nm may be attributed to the diameter of tropocollagen molecules, isolated or associated (Dubey and Tomar, 2009) or to the average thickness of mineral hydroxyapatite in archeological bone (5.16 nm) which due to remineralization may be larger than the mean value of non archeological bone (3.49 nm) (Wess et al., 2001a,b). The peaks at 1.2 and 2.7 nm could be due to smaller fractions. Still, this point illustrates the difficulty of interpretation of SAXS measurements in systems as complex as bone. Indeed, SAXS is due to electron density contrast among hydroxyapatite particles, collagen or pores and the surrounding medium. Thus, the peak at 2.7 nm may be attributed, as well, to the average size of hydroxyapatite crystallites, which turns out to be 2.3–2.8 nm (Hiller and Wess, 2006) or even 3.49 nm (Wess et al., 2001a, b). The SAXS curve corresponds mostly to the highest contrast, which in this case, is the electron density contrast between the mineral and collagenous components; then, the peak corresponds mostly to the size of the hydroxyapatite crystals.

However, when disease or taphonomy generates some microporosity, the interpretation may not be clear. The diseased samples of this group (MC-tibia-s and MT-metac-s) do not show any significant differences from healthy bone; hence, the measured heterogeneity size distributions correspond to the nanometrical features of bone and do not reflect the changes in porosity. Therefore, the use of the word "heterogeneities" in this case is justified as such heterogeneities are microfibrils, tropocollagen molecules and mostly hydroxyapatite crystals typical of bone, those heterogeneities do not depend on taphonomy or treponematosis. It has been already shown how constant are the composition and structure of bone (Piga et al., 2013).

3.3. Scanning electron microscopy

Fig. 4 is a micrograph of the seemingly healthy bone from la Candelaria, MC-fibula-h; the *feather-like* texture is typical of bone surfaces and it has been often observed in other healthy bones (Weiner and Traub, 1992; Pijoan et al., 2007; Trujillo-Mederos et al., 2012; Fantner et al., under review). At a lower magnification a large pore is evident ca. 30 μm.

In the corresponding bone with pathological alterations, MC-tibia-s (Fig. 5), a large pore ca. 8 μm and smaller pores ca. 0.3 μm are evident. Still, instead of a feather-like surface a smooth surface with fading spheres ca. 1 to 2 μm on top is evident. This surface is definitely different from the one observed in sample MC-fibula-h.

The surface of the healthy bone from Tlatelolco, MT-tibia-h, is smooth with cracks (Fig. 6). The feather-like morphology reported for sample MC-fibula-h is not observed. Large pores ca. 15 and 90 μm are present. The surface seems to be covered by a layer of a plastic and smooth material, most probably clay or a residue of collageneous material coming from dried skin. Note that the specific surface area of these samples is very low and, if the contribution of clay was significant, it would be much higher as the specific surface area of illite, for instance, is ca. 80 m^2/g or for montmorillonite ca. 60 m^2/g (Macht et al., 2011).

The corresponding surface of the diseased sample from Tlatelolco is very peculiar as several morphologies were evident. In Fig. 7, the very large pore is ca. 60 μm and the small ones are ca. 1 μm. The surface is covered by filaments, evident in Fig. 8, which emerge from the small pores. Their diameter is ca. 0.1 μm and reproduces those reported by Trujillo-Mederos et al. (2012) for bones boiled in salted water.

4. Discussion

The results exposed previously seem contradictory. Gas adsorption isotherms were only obtained in Tlatelolco samples; gas is not adsorbed by the other samples, i.e. la Candelaria materials were not porous. But, SAXS technique showed that the heterogeneities in all samples are comprised between 0.8 and 4.5 nm. The bone surface was smooth in the tibia samples MT-tibia-h, MC-tibia-s, independently of the origin or the alterations. The sample from Tlatelolco MT-metacarpal-s presents collagen filaments on the surface and sample MC-fibula-h has the expected texture in a seemingly healthy bone. No correlation between those results and treponematosis is evident (Table 3).

Table 3
Comparison of results obtained by gas adsorption, SAXS and SEM.

Sample	Gas adsorption (S in $m^2/g \pm 0.7$) (V_p in $cm^3/g \pm 0.01$)	SAXS (diameter values from size distribution curves in nm ± 0.3)	SEM
MC-tibia-s	S (m^2/g) <2	Broad distribution from 0.8 to 4.5 nm	Smooth surface
MT-tibia-h	S (m^2/g) = 35 Vp (cm^3/g) = 0.13 d = 7.42 nm	Broad distribution from 0.8 to 4.5 nm	Smooth surface
MT-metacarpal-s	S (m^2/g) = 22 Vp (cm^3/g) = 0.05 d = 5.44 nm	Broad distribution from 0.8 to 4.5 nm	Filaments
MC-fibula-h	S (m^2/g) <2	Broad distribution from 0.8 to 4.5 nm	Feather-like texture

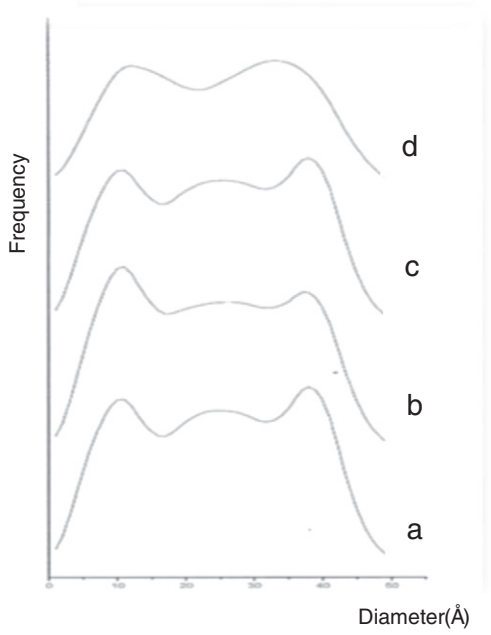

Fig. 3. Pore size distributions of the Mesoamerican samples (frequency vs diameter in Å). From bottom to top: a) MC-fibula-h, b) MC-tibia-s, c) MT-tibia-h, and d) MT-metac-s.

The bone porous system is a hierarchical complex structure. Two ranges of sizes may be distinguished, on the one hand, a micrometric porosity (Haversian canals) and, on the other, a nanometric one corresponding to lacunae and canaliculi. In gas adsorption characterization, MC-tibia-s and MC-fibula-h, both from la Candelaria, were not porous, i.e. that the nanometric porous system, which is the responsible for the high specific surfaces, was not reached by nitrogen. The organic compounds formed during natural mummifying then, most probably, occlude access to lacunae and canaliculi. As Tlatelolco burials were not mummified such process did not occur; thus, they present higher specific surface areas, 35 and 22 m^2/g. Reported specific surface values vary from 20 to 100 m^2/g (Smith et al., 2008; Figueiredo et al., 2010). These values reproduce those reported in previous works for archeological bones (Hedges et al., 1995; Bosch et al., 2011). Remember that the surface area of fresh bone is 85–170 m^2/g (Misra et al., 1978) and that in archeological bones a loss of microporosity and increase in macroporosity has been reported (Hedges et al., 1995). Using the correlation proposed by Nielsen-Marsh and Hedges (1999) the amount of protein left in the Tlatelolco bones would be 3.5% for the MT-metacarpal-s and more than 5% for the MT tibia-h. As bone degrades, the amount of collagen diminishes (Hedges and Law, 1989), but collagen itself also degrades so that it is no longer well-defined chemically; therefore, sample MT-metacarpal-s is more degraded.

The size distributions obtained using SAXS correspond to the heterogeneities in the samples. Only the last peak of the distribution could be

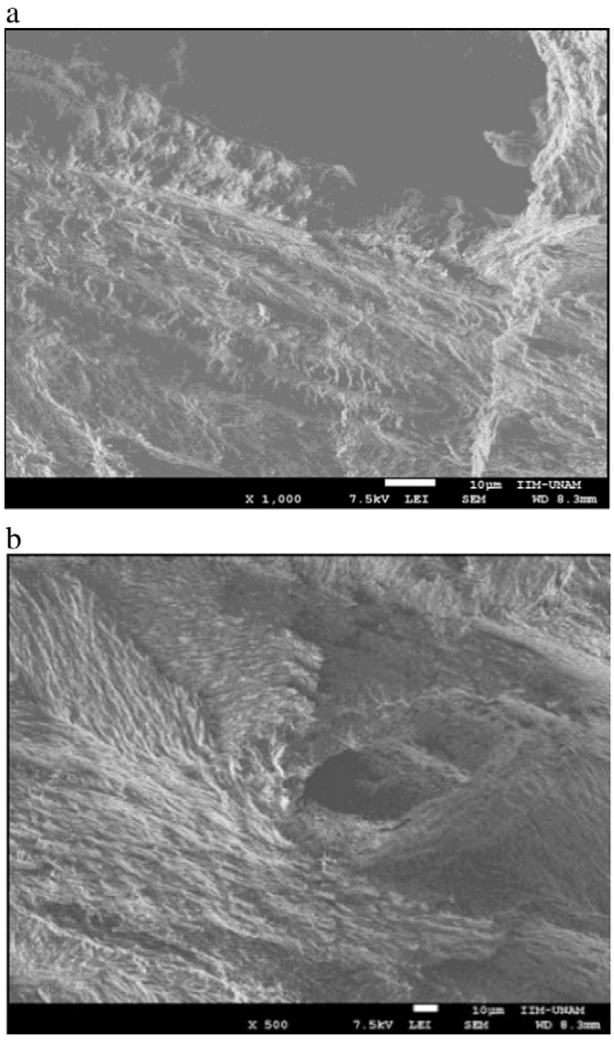

Fig. 4. Surface morphology of the seemingly healthy bone from la Candelaria, MC-fibula-h, at two magnifications: a) ×1000 and b) ×500.

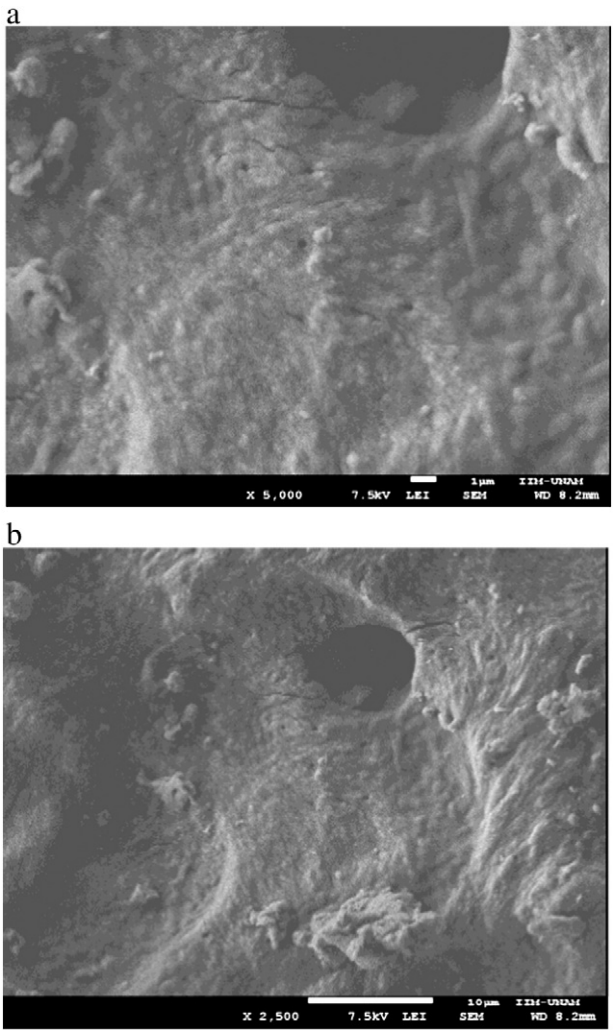

Fig. 5. Surface morphology of the pathologically altered bone from la Candelaria, MC-tibia-s, at two magnifications: a) ×5000 and b) ×2500.

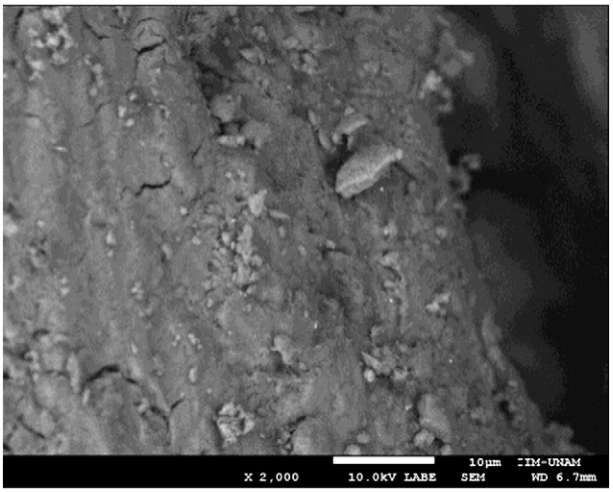

Fig. 6. Surface morphology of the seemingly healthy bone from Tlatelolco, MT-tibia-h, at ×2000 magnification.

attributed to pores as it corresponds to the sizes determined in the Tlatelolco samples with gas adsorption. Still, it is the same in all samples, and gas adsorption showed that the samples from La Candelaria were definitely different from those of Tlatelolco. This disagreement can be explained proposing closed pores in La Candelaria samples as suggested by the scanning electron microscopy images. Open pores are detected by gas adsorption which is a surface technique but small angle X ray scattering which is a bulk technique includes closed pores (bubbles for instance). The remaining part of the distribution must be due to solid materials, such as the components of bone or clays from soil. Still, the sizes correspond to residues of collagen fibrils. Collagen fibrils are, indeed, 10 nm diameter and 300 nm length, depending on the type of collagen. From control modern bones, the average thickness of mineral compound in archeological bone has been evaluated to be 5.16 nm and 3.49 nm in non-archeological control bone. The spread of the values reveals that a wide range of crystal sizes can be attained by mineral remodeling over time. Hence, gas adsorption measurements with SEM and SAXS provide a clear picture of bone morphology.

Porosity due to treponematosis may not be evident if determined by gas adsorption as mummifying conditions may occlude it. In this case, surface morphology revealed by SEM indicates that the surface is smooth and flat. Instead, bones from Tlatelolco present the expected specific surface areas of archeological bones. Still, SEM shows that the small amount of collagen migrates to the surface due to a salted water environment. This result is most interesting as the exiting collagen does not block pores (which are then detected by gas adsorption) in a mechanism whose result is similar to a boiling process in salted water. Such similarity has been already mentioned in previous works (Collins et al., 2002; Roberts et al., 2002; Bosch et al., 2011; Trujillo-Mederos et al., 2012).

5. Conclusion

The differences between human pathological and healthy bones may be clear macroscopically. Porosity can be an indicator of treponematosis. However, those criteria may be masked by taphonomy. In the present work we found that salted water may affect the morphology of bone as much as if it was boiled in seawater. Bone pores are occluded in the La Candelaria cave samples. This result is important since it is known that this cultural group has treponematosis and that porosity is one of the changes caused by this infection. Physical characterization techniques were used to show that the macroscopic morphology is reproduced at a nanometric level. It is difficult to separate, in archeological human bones, the effect of disease and taphonomy.

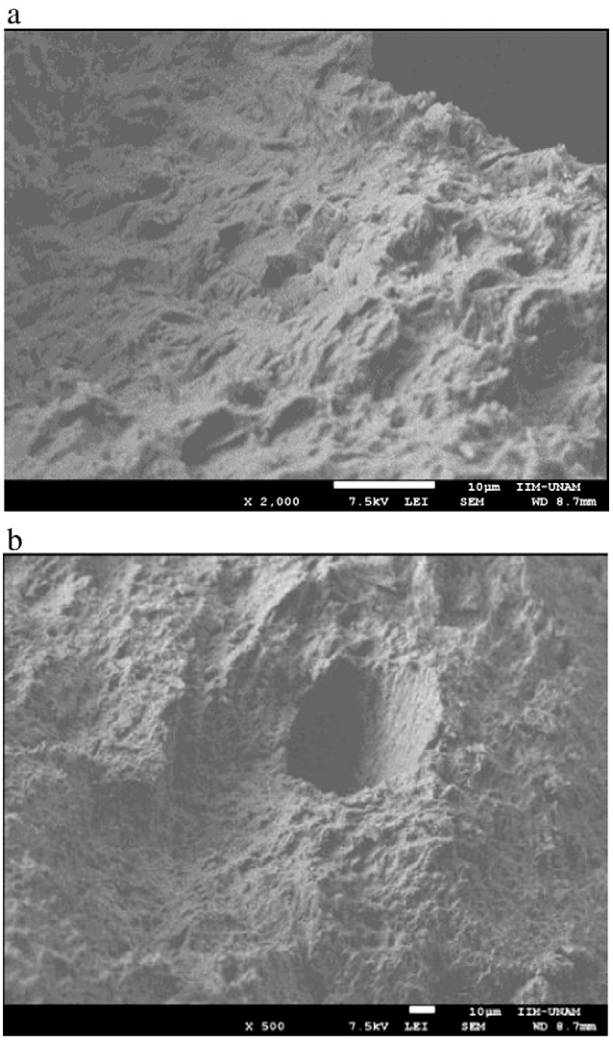

Fig. 7. Surface morphology of the pathological bone from Tlatelolco, MT-metacarpal-s, at two magnifications: a) x 2000 and b) x 500.

Furthermore, the usual technique to determine porosity in materials (gas adsorption), complemented with scanning electron microscopy and small angle X-ray scattering, reveals that porosity is still a relative

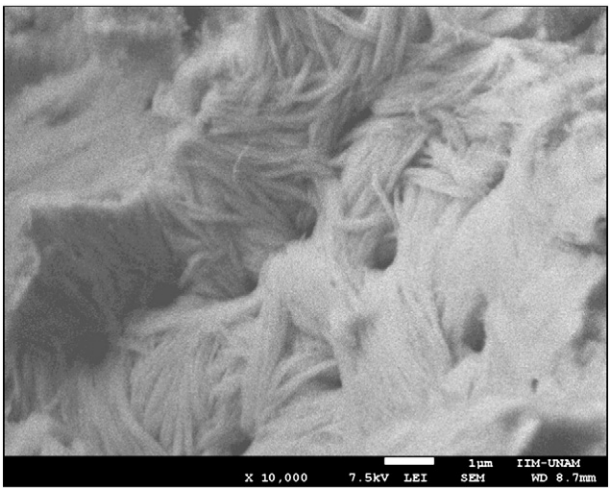

Fig. 8. Surface morphology of the pathological bone from Tlatelolco, MT-metacarpal-s, at high magnification: ×10,000.

value which depends, not only on the features of bone sample, but on the characterization technique.

Acknowledgments

The technical work of O. Novelo, V. H. Lara and M. H. García-Rosero in electron microscopy, X-ray diffraction and gas adsorption, respectively, is gratefully acknowledged. I. Leboreiro took the bone samples; his work was essential for this study.

References

Bosch, P., Alemán, I., Moreno-Castilla, C., Botella, M., 2011. Boiled *versus* unboiled, a study on Neolithic and contemporary human bones. J. Archaeol. Sci. 38, 2561–2570.

Cervini-Silva, J., Palacios, E., Muñoz, M. de L., Del Angel, P., Montoya, J.A., Ramos, E., López, F., Romano Pacheco, A., 2013. Cinnabar-preserved bone structures from primary osteogenesis and fungal signatures in ancient human remains. Geomicrobiol J. 30, 566–577.

Collins, M.J., Nielsen-Marsh, C.M., Hiller, J., Smith, C.I., Roberts, J.P., Prigodich, R.V., Wess, T. J., Csapò, J., Millard, A.R., Turner-Walker, G., 2002. The survival of organic matter in bone: a review. Archaeometry 44, 383–394.

Craievich, A., 2002. Synchrotron SAXS studies of nanostructured materials and colloidal solutions. A review. Mater. Res. São Carlos http://dx.doi.org/10.1590/S1516-14392002000100002 (consulted on March 10, 2014).

Dubey, D.K., Tomar, V., 2009. Effect of tensile and compressive loading on hierarchical strength of idealized tropocollagen-hydroxyapatite biomaterials as a function of chemical environment. J. Phys. Condens. Matter 21, 25103–25116.

El Shafei, G.M., Philip, C.A., Moussa, N.A., 2004. Fractal analysis of hydroxyapatite from nitrogen isotherms. J. Colloid Interface Sci. 277, 410–416.

Fantner, G.E., Rabinovych, O., Schitter, G., Thurner, P., Kindt, J.H., Finch, M.M., Weaver, J.C., Golde, L.S., Morse, D.E., Lipman, E.A., Rangelow, I.W., Hansma, P.K., 2014w. Hierarchical interconnections in the nano-composite material bone: fibrillar cross-links resist fracture on several length scales. Compos. Sci. Technol. (under review, pdf).

Figueiredo, M., Henriques, J., Martins, G., Guerra, F., Judas, F., Figueiredo, H., 2010. Physicochemical characterization of biomaterials commonly used in dentistry as bone substitutes—comparison with human bone. J. Biomed. Mater. Res. B Appl. Biomater. 92B, 409–419.

Glatter, O., Gruber, K., 1993. Indirect transformation in reciprocal space: desmearing of small-angle scattering data from partially ordered systems. J. Appl. Crystallogr. 26, 512–518.

Guinier, A., Fournet, G., 1955. Small Angle Scattering of X-rays. Wiley, New York.

Gutierrez, M.A., 2001. Bone diagenesis and taphonomic history of the Paso Otero bone bed, Pampas of Argentina. J. Archaeol. Sci. 28, 1277–1290.

Hackett, C.J., 1976. Diagnostic criteria of syphilis, yaws and treponarid (treponematoses) and some other diseases in dry bones. Springer, Berlin.

Hedges, R.E.M., Law, I.A., 1989. Radiocarbon dating of bone. Appl. Geochem. 4, 249–253.

Hedges, R.E.M., Millard, A.R., Pike, A.W.G., 1995. Measurements and relationships of diagenetic alteration of bone from three archaeological sites. J. Archaeol. Sci. 22, 201–209.

Hiller, J.C., Wess, T.J., 2006. The use of small-angle X-ray scattering to study archaeological and experimentally altered bone. J. Archaeol. Sci. 33, 560–572.

Kataoka, M., Hagihara, Y., Mihara, K., Goto, Y., 1993. Molten globules of cytocrome c studied by the small angle X-ray scattering. J. Mol. Biol. 229, 591–596.

Kataoka, M., Flanagan, J.M., Tokunaga, F., Engelman, D.M., 1994. Use of X-ray solution scattering for protein folding study in synchrotron radiation. In: Chanse, B., Deisenhofer, J., Ebashi, S., Goodhead, D.T., Huxley, H.E. (Eds.), The Biosciences 4. Clarendon Press, Oxford, U.K., pp. 87–92.

Labastida Pólito, A., Piña Barba, C., Tello Solís, S., 2006. Collagen Type I scaffolds for use in medicine. AIP Conf. Proc. 854, 129.

Macht, F., Eusterhues, K., Pronk, G.J., Totsche, K.U., 2011. Specific surface area of clay minerals: comparison between atomic force microscopy measurements and bulk-gas (N_2) and -liquid (EGME) adsorption methods. Appl. Clay Sci. 53, 20–26.

Mansilla, J., Pijoan, C., 2005. Treponematosis in ancient Mexico. In: Powell, L.M., Cook, C.D. (Eds.), The myth of syphilisThe Natural History of Treponematosis in North America. University Press of Florida, Gainsville, FL, pp. 368–385.

Mansilla, J., Solís, C., Chávez-Lomeli, M.E., Gama, J.E., 2003. Analysis of colored teeth from Precolumbian Tlatelolco: postmortem transformation or intravitam processes? Am. J. Phys. Anthropol. 120, 73–82.

Mays, S., 2008. Metabolic bone disease. In: Pinhasi, R., Mays, S. (Eds.), Advances in Human Palaeopathology. John Wiley & Sons, West Sussex, UK, pp. 214–251.

Misra, D.N., Bowen, R.L., Mattamal, G.J., 1978. Surface area of dental enamel, bone, and hydroxyapatite: chemisorption from solution. Calcif. Tissue Res. 26, 139–142.

Nielsen-Marsh, C.M., Hedges, R.E.M., 1999. Bone porosity and the use of mercury intrusion porosimetry in bone diagenesis studies. Archaeometry 41, 165–174.

Ortner, D.J., 2008. Differential diagnosis of skeletal lesions in infectious disease. In: Pinhasi, R., Mays, S. (Eds.), Advances in Human Palaeopathology. John Wiley & Sons, Chichester (England), pp. 191–214.

Piga, G., Solinas, G., Thompson, T.J.U., Brunetti, A., Malgosa, A., Enzo, S., 2013. Is X-ray diffraction able to distinguish between animal and human bones? J. Archaeol. Sci. 40, 778–785.

Pijoan, C.Ma., Mansilla, J., Leboreiro, I., Lara, V.H., Bosch, P., 2007. Thermal alterations in archaeological bones. Archaeometry 49, 713–727.

Pinhasi, R., Mays, S. (Eds.), 2008. Advances in Human Palaeopathology. John Wiley & Sons, Chichester (England).

Powell, L.M., Cook, C.D., 2005. Treponematosis: inquiries into the nature of a Protean disease. In: Powell, L.M., Cook, C.D. (Eds.), The myth of syphilisThe Natural History of Treponematosis in North America. University Press of Florida, Gainsville, FL, pp. 9–62.

Roberts, S.J., Smith, C.I., Millard, A., Collins, M.J., 2002. The taphonomy of cooked bone: characterising boiling and its physico-chemical effects. Archaeometry 44, 485–494.

Rouquerol, J., Rouquerol, F., Sing, K.S.W., 1999. Adsorption by Powders and Porous Solids: Principles, Methodology and Applications. Academic Press, San Diego, U.S.A.

Sing, K., 2001. The use of nitrogen adsorption for the characterization of porous materials. Colloids Surf. A Physicochem. Eng. Asp. 187–188, 3–9.

Smith, C.I., Faraldos, M., Fernández-Jalvo, Y., 2008. The precision of porosity measurements: effects of sample pre-treatment on porosity measurements of modern and archaeological bone. Palaeogeogr. Palaeoclimatol. Palaeoecol. 266, 175–182.

Trujillo-Mederos, A., Alemán, I., Botella, M., Bosch, P., 2012. Changes in human bones boiled in seawater. J. Archaeol. Sci. 39, 1072–1079.

Turner-Walker, G., 2008. The chemical and microbial degradation of bones and teeth. In: Pinhasi, R., Mays, S. (Eds.), Advances in Human Palaeopathology. John Wiley & Sons, Chichester (England), pp. 3–29.

Vinogradova, E., Moreno, A., Lara, V.H., Bosch, P., 2003. Multi-fractal imaging and structural investigation of silica hydrogels and aerogels. Silicon Chem. 2, 247–251.

Waldron, T., 2009. Palaeopathology. Cambridge University Press.

Walker, P.L., Bathurst, R.R., Richman, R., Gjerdrum, T., Andrushko, V.A., 2009. The causes of porotic hyperostosis and criba orbitalia: a reappraisal of the iron-deficiency anemia hypothesis. Am. J. Phys. Anthropol. 139, 109–125.

Wang, X., Ni, Q., 2003. Determination of cortical bone porosity and pore size distribution using a low field pulsed NMR approach. J. Orthop. Res. 21, 312–319.

Weiner, S., Traub, W., 1992. Bone structure: from ångströms to microns. FASEB J. 6, 879–885.

Wess, T.J., Drakopoulos, M., Snigirev, A., Wouters, J., Paris, O., Fratzl, P., Collins, M., Hiller, J., Nielsen, K., 2001a. The use of small-angle X-ray diffraction studies for the analysis of structural features in archaeological samples. Archaeometry 43, 117–129.

Wess, T.J., Alberts, I., Hiller, J., Drakopoulos, M., Chamberlain, A.T., Collins, M., 2001b. Microfocus small angle X-ray scattering reveals structural features in archaeological bone samples: detection of changes in bone mineral habit and size. Calcif. Tissue Int. 70, 103–110.